GMR
The Original

REMODELING THE TUMOR MICROENVIRONMENT: INTRATUMORAL PIRFENIDONE SENSITIZES MURINE TUMORS TO ANTI-PD-1 THERAPY

CH Sandeep Reddy[1], Lalitha Repudi[2*]

[1]Research Scholar, Department of Pharmacy, Chaitanya Deemed to be University (Deemed to be University), Gandipet, Himayat Nagar, Moinabad, Hyderabad, Telangana, India, ch.sandeep27@gmail.com
[2*]M. Pharm., Ph.D, Associate Professor, Chaitanya Deemed to be University , Himayath Nagar, Moinabad, Hyderabad, Telangana, India, Email: repudilalitha@gmail.com
*Corresponding Author: Dr. Lalitha Repudi, Email: repudilalitha@gmail.com

Abstract
The tumor microenvironment (TME) represents a critical barrier to effective cancer immunotherapy. Pirfenidone (PFD), an anti-fibrotic agent, has shown promise in modulating the immunosuppressive TME by inhibiting the TGF-β pathway. Objective: To evaluate the antitumor efficacy of intra-tumoral pirfenidone (PFD), an anti-fibrotic agent with tumor microenvironment (TME)-modulating properties, alone and in combination with anti-PD-1 antibody therapy in syngeneic CT26 colon carcinoma and 4T1 breast cancer models. Methods: CT26 colon carcinoma and 4T1 breast cancer-bearing mice were treated with intra-tumoral pirfenidone either as monotherapy or in combination with anti-PD-1 antibodies. Tumor growth was monitored throughout the study. Results: Pirfenidone monotherapy attenuated tumor growth in both CT26 and 4T1 tumor models. Combination treatment with pirfenidone and anti-PD-1 antibodies resulted in significantly greater tumor growth inhibition compared with monotherapy. Furthermore, tumors from the combination-treated group exhibited enhanced antitumor immune responses and favorable remodeling of the tumor microenvironment. These findings suggest that pirfenidone-mediated TME remodeling enhances the efficacy of checkpoint inhibitors and warrants further investigation as a combination immunotherapy strategy.

KEYWORDS: pirfenidone, PD-1 antibody, tumor microenvironment, immunotherapy, CT26, 4T1, TGF-β signaling

INTRODUCTION

Immune checkpoint inhibitors targeting the programmed cell death protein-1 (PD-1)/programmed death-ligand 1 (PD-L1) pathway have transformed the treatment landscape for multiple cancers by restoring anti-tumor T-cell responses[1]. Despite their remarkable clinical success, a substantial proportion of patients either fail to respond initially or develop acquired resistance during treatment[2]. Increasing evidence indicates that the tumor microenvironment (TME) plays a critical role in limiting the efficacy of checkpoint blockade. In particular, tumors characterized by extensive fibrosis, dense stromal architecture, and immunosuppressive cellular populations often exhibit poor infiltration of cytotoxic T lymphocytes and are commonly referred to as immunologically “cold” tumors. These tumors remain a major challenge in cancer immunotherapy and highlight the need for therapeutic strategies capable of remodeling the TME to support effective anti-tumor immune responses[3–5]

Transforming growth factor-beta (TGF-β) is a key regulator of tumor-associated fibrosis and immune suppression. Elevated TGF-β levels promote activation of cancer-associated fibroblasts (CAFs), extracellular matrix (ECM) deposition, epithelial-mesenchymal transition, and recruitment of immunosuppressive cell populations such as myeloid-derived suppressor cells (MDSCs) and regulatory T cells [6,7]. The resulting fibrotic and desmoplastic stroma acts as both a physical and functional barrier that restricts immune cell infiltration into the tumor core. Consequently, T cells remain excluded from tumor parenchyma, limiting the therapeutic benefit of PD-1/PD-L1 blockade. Since TGF-β-mediated immune exclusion represents a mechanism distinct from checkpoint signaling, targeting the fibrotic microenvironment may provide an effective strategy to overcome resistance to immunotherapy[8,9].

Pirfenidone is an orally available pyridine-derived antifibrotic agent approved for the treatment of idiopathic pulmonary fibrosis. Its primary mechanism involves inhibition of TGF-β signaling, resulting in suppression of fibroblast activation, collagen synthesis, inflammatory cytokine production, and tissue fibrosis[10,11]. In addition to its established antifibrotic effects, recent studies have demonstrated that pirfenidone possesses broader anticancer properties, including inhibition of tumor cell proliferation, modulation of tumor-promoting growth factors, and suppression of stromal remodeling. Pirfenidone has also been shown to reduce CAF-mediated immunosuppression and alter cytokine networks within the TME, thereby promoting a more favorable environment for anti-tumor immunity[8,12,13].

The ability of pirfenidone to reduce ECM deposition and stromal rigidity is particularly important in solid tumors, where dense fibrotic barriers impede immune cell trafficking and therapeutic drug penetration. By attenuating fibrosis and lowering interstitial pressure within tumors, pirfenidone may enhance the infiltration and activity of cytotoxic T lymphocytes. Furthermore, inhibition of TGF-β signaling may reduce the accumulation of MDSCs and other suppressive

immune cell populations, thereby restoring immune surveillance and augmenting the efficacy of checkpoint inhibitors[14,15] These effects suggest that pirfenidone has the potential to convert immunologically "cold" tumors into more immune-responsive tumors.

The combination of pirfenidone with PD-1 blockade offers a mechanistically rational approach for improving anti-tumor efficacy. While anti-PD-1 antibodies reactivate exhausted T cells, pirfenidone may simultaneously remodel the tumor stroma, reduce immune suppression, and facilitate immune-cell access to the tumor core. Such complementary actions could potentially overcome primary resistance to immunotherapy and enhance therapeutic responses.

Therefore, the present study evaluated the anti-tumor effects of intratumoral pirfenidone administration, alone and in combination with anti-PD-1 therapy, in the syngeneic CT26 colorectal carcinoma and 4T1 breast carcinoma mouse models. We hypothesized that local delivery of pirfenidone would remodel the tumor microenvironment by attenuating fibrosis and suppressing TGF-β-driven immunosuppressive pathways, thereby enhancing immune-cell infiltration and potentiating the anti-tumor activity of PD-1 blockade. This combinatorial strategy may represent a promising approach for improving immunotherapy outcomes in tumors characterized by stromal desmoplasia and immune exclusion.

MATERIALS AND METHODS

Animals

Female BALB/c mice (6-8 weeks old) were obtained from the G.V Reasearch platform (Hyderabad, India). All procedures were approved by the Institutional Animal Care and Use Committee (IAEC no: IAEC/AUR/2023/11/52/PH/SYNG/CH/116/M/M/F-84 and IAEC/AUR/2024/12/56/PH/SYNG/SM/175/M/F-100) and performed according to institutional guidelines. Mice were maintained under standard conditions with controlled temperature (23 ± 3°C), humidity (50 ± 20%), and 12-hour light-dark cycle. Food and water were provided ad libitum.

Tumor Cell Lines and Culture

CT26 colon carcinoma(CRL-2638) and 4T1 breast cancer cell line(CRL-2539) were obtained from ATCC and cultured in RPMI 1640 medium (Gibco, USA) supplemented with 10% fetal bovine serum and 1% penicillin-streptomycin at 37°C in 5% CO_2. Cell expansion was carried out in T-175cm2 flasks. After the final step of splitting, cells were processed for injection when the cells reach exponential phase. Cells were trypsinized with 1x Trypsin-EDTA solution and cell suspension from T-175cm2 flask was centrifuged at 1200 rpm for 5 minutes to obtain cell pellet and then re-suspended in media and counted using hemocytometer. Based on the cell count cells were re-suspended in RPMI-1640 plain media at a final concentration of 10x10^6 cells/mL..

Tumor Inoculation and Treatment Groups

Mice were inoculated subcutaneously with 100 µL of CT26 or 4T1 cells (1 × 106 cells/mL)cells in the right flank using 27guage 1mL BD Tuberculin syringe. Tumors were allowed to establish for 5-10 days (mean volume ~50-80 mm^3) before treatment initiation. Mice were randomized into four treatment groups with n=8 for CT26 and n=6 for 4T1 tumors using randomization tool (RandoMice):

- Group 1: Vehicle control (10% DMSO in PBS intratumoral injection)
- Group 2: Pirfenidone monotherapy (1 mg/mouse intratumoral, twice weekly for 3 weeks)
- Group 3: Anti-PD-1 antibody monotherapy (200 µg intraperitoneal, twice weekly for 3 weeks[16])
- Group 4: Combination therapy (pirfenidone 1 mg/mouse intratumoral + anti-PD-1 antibody 200 µg intraperitoneal, both twice weekly for 3 weeks)

Treatments

Following randomization, animals were administered the respective treatments twice weekly for 3 weeks. Pirfenidone(HY-B0673, MedChemExpress, NJ, USA) was dissolved in DMSO and further diluted with PBS to a final concentration of 50 mg/mL. Animals in Groups G2 and G4 received either vehicle or Pirfenidone (20 µL) via intratumoral administration. Animals in Groups G3 and G4 received either dilution buffer(InVivoPure pH 7.0 dilution buffer) or Anti-mouse PD-1 (CD279) control (BP0146, InVivoPlus, 9.78 mg/mL) at 1 mg/mL, 200 µL/mouse via the intraperitoneal (i.p.) route. Correspondingly, animals in Groups G1 and G2 received dilution buffer via i.p. injection, while animals in Groups G1 and G3 received 20 µL of 10% DMSO in PBS intratumorally to match the treatment groups.

Measurement of Tumor Growth and Survival

Tumor volume was measured using digital caliper(Fowler sylvac) twice weekly and calculated using the formula: TV = (length × $width^2$)/2. Animals were planned to euthanize when tumors reached 2500 mm^3. Overall survival was recorded as the time from tumor inoculation to death or humane endpoint.

Study termination, tumor and organ collection

At the end of the study , mice were euthanized and tumor tissues were excised, weighed. For 4T1 study tumor samples were flash-frozen for molecular analysis or fixed in 10% formalin for subsequent histopathological evaluation [17]. Additionally lung and liver tissues from animals administered 4T1 cells were also collected and fixed in 10% formalin for metastasis assessment.

Histopathology
Formalin fixed tissues were embedded in paraffin, and cut into 5 µm sections. These sections were then stained with haematoxylin and eosin dye for structural assessment and metastasis. For Lung tissue total no of foci were counted per slide at 40X magnification and for liver tissue total foci were counted at 100X magnification using microscope(Nikon), diameter of Lung foci was measured using NIS elements AR software.

Quantitative Real-Time PCR
Total RNA was isolated from ~50 mg of Tumor using the RNeasy Mini Kit (Qiagen). Tumor tissues were homogenized in TRI Reagent(T9424, Sigma), followed by chloroform extraction and centrifugation to separate the aqueous RNA phase. The aqueous phase was mixed with 70% ethanol and loaded onto an RNeasy spin column. After sequential washes with RW1 and RPE buffers, RNA was eluted with RNase-free water. The concentration and purity of the isolated RNA was determined using a NanoDrop(Thermo)). Complementary DNA (cDNA) was synthesized from 2 µg of total RNA using the High-Capacity cDNA Reverse Transcription Kit (Applied Biosystems) according to the manufacturer's instructions. A reverse transcription master mix, RNase inhibitor, and nuclease-free water was prepared and combined with the RNA template to obtain a final reaction volume of 20 µL. Reverse transcription was performed in a thermal cycler under optimized cycling conditions recommended by the manufacturer., Quantitative RT-PCR was performed on an ABI 7500 Fast system (Applied Biosystems, USA) using gene-specific primers for TGF-β, IL-6, TNF-α, IFN-γ, IL-12, and GAPDH (endogenous control). cDNA samples were diluted to a final concentration of 16 µg/mL, and gene-specific primers were diluted to 10 µM using nuclease-free water. The reaction components were added to the PCR wells in duplicate, as described in the table below. Quantitative real-time PCR (qRT-PCR) was performed with an initial polymerase activation step at 95°C for 10 minutes, followed by 40 cycles of denaturation at 95°C for 15 seconds and annealing/extension at 60°C for 1 minute. Gene expression levels were normalized to the selected housekeeping gene. Relative mRNA expression was determined using the comparative Ct (2^-ΔΔCt) method, where ΔCt values were calculated by normalizing target gene Ct values to the housekeeping gene Ct values. ΔΔCt values were then obtained by comparing the ΔCt of treatment groups with that of the control group, and relative fold changes in gene expression were expressed as 2^-ΔΔCt

PCR Master Mix (µL) (Syber Green)	10 µM Forward Primer (µL)	10 µM Reverse Primer (µL)	cDNA Template (µl)	Nucleus free Water (µL)	Total Volume (µL)	Template (ng) in 20µl rxn
10	0.8	0.8	5	3.4	20	40

Primer details

TNF-α	ATGAGCACTGAAAGCATGATCC --- Forward
	GAGGGCTGATTAGAGAGAGGTC --- Reverse
IL-6	CCTCTCTGCAAGAGACTTCCAT-- Forward
	AGTCTCCTCTCCGGACTTGT-- Reverse
TGF-β1	ACAGCAGGGATAACACAC-- Forward
	GCAATAGTTGGTGTCCAG-- Reverse
IFN-γ	AAAGAGATAATCTGGCTCTGC-- Forward
	GCTCTGAGACAATGAACGCT-- Reverse
IL-12a	ACGAGAGTTGCCTGGCTACTAG-- Forward
	CCTCATAGATGCTACCAAGGCAC-- Reverse
GAPDH	CATCACTGCCACCCAGAAGACTG-- Forward
	ATGCCAGTGAGCTTCCCGTTCAG-- Reverse

Tumor cytokines
Tumor lysates were prepared in lysis buffer (89900, Thermo Fisher Scientific) containing protease inhibitors(78420, Thermo Fisher Scientific) Cytokine levels of TNF-α(DY410, R&D Systems), IL-6 (DY406, R&D Systems), TGF-β (DY1679, R&D Systems)and IFN-γ(DY485, R&D systems) in tumor lysates were quantified according to the manufacturer's instructions and were normalized to total protein estimated using Bradford reagent(B6916, Sigma Aldrich)

Statistical Analysis
Statistical analyses were performed using GraphPad Prism(9.1.2). All data are presented as mean ± standard deviation (SD), and statistical significance was established at $p < 0.05$.To evaluate longitudinal changes in tumor growth curves across multiple days, two-way repeated measures analysis of variance (ANOVA) was applied time was treated as a repeated factor and treatment group as a between-subject factor. For single-endpoint metrics evaluated at day 21 differences across groups were analyzed using an ordinary one-way analysis of variance (ANOVA)., Dunnett's post-hoc multiple comparisons test was systematically applied to determine specific statistical differences between individual treatment groups and the designated baseline vehicle control group for all parameters..

RESULTS

Pirfenidone Monotherapy Attenuates Tumor Growth In Ct26 And 4T1 Models

Intratumoral pirfenidone administration significantly reduced tumor growth compared to vehicle control in both CT26 (44% growth inhibition, $p < 0.001$) and 4T1 (32% growth inhibition, $p < 0.05$) models. In the CT26 model, 1/8 mice receiving pirfenidone achieved complete regression with sustained tumor-free status throughout the study.

Anti-PD-1 Antibody Monotherapy Shows Variable Efficacy

CT26 tumors demonstrated greater sensitivity to PD-1 blockade (53% inhibition) with 1/8 mice achieved complete regression. In contrast, 4T1 tumors exhibited resistance to anti-PD-1 monotherapy, with no regressions observed, consistent with multiple reports documenting poor responsiveness or limited antitumor effects of PD-1 blockade in this syngeneic model [18–21].

Combination Therapy Demonstrates Synergistic Antitumor Effects

The combination of intratumoral pirfenidone with anti-PD-1 antibodies produced superior antitumor effects compared to monotheraies:

- **CT26 model:** Combination therapy achieved 70% tumor growth inhibition ($p < 0.0001$ vs. control)
- **4T1 model:** Combination therapy achieved 58% tumor growth inhibition ($p < 0.0001$ vs. control)

In the CT26 model, 3/8 mice receiving combination therapy achieved complete tumor regression with durable responses.

Pirfenidone Modulates Tumor Microenvironment Cytokine Expression in 4T1 tumor model

Quantitative RT-PCR analysis of tumor tissue revealed distinct cytokine profiles by treatment group:

Table 2: Gene expression fold-change (relative to control). *p < 0.05 vs. control; **p < 0.01 vs. control

Cytokine	Control	Pirfenidone	Anti-PD-1	Combination
TGF-β	1.0 ± 0.14	0.38 ± 0.05	0.85 ± 0.12	0.22 ± 0.03**
IL-6	1.0 ± 0.26	0.52 ± 0.08*	0.68 ± 0.09	0.31 ± 0.04**
TNF-α	1.0 ± 0.28	1.1 ± 0.15	1.8 ± 0.20*	2.3 ± 0.25**
IFN-γ	1.0 ± 0.14	1.5 ± 0.18	2.1 ± 0.22*	3.2 ± 0.30**
IL-12	1.0 ± 0.10	1.3 ± 0.16	2.0 ± 0.19*	2.8 ± 0.24**

Pirfenidone monotherapy significantly suppressed TGF-β and IL-6 expression compared to controls, indicating TME remodeling toward a less immunosuppressive phenotype. Combination therapy further reduced immunosuppressive cytokines while promoting pro-inflammatory cytokines (TNF-α, IFN-γ, IL-12) associated with anti-tumor immunity.

Pirfenidone Reduces Metastasis in 4T1 tumor model

Histopathological analysis of lung tissue revealed a significant decrease in the number of 4T1 tumor nodules in mice treated with Pirfenidone and combination therapy compared to those receiving PD1 antibody or vehicle control. This reduction in metastatic burden suggest that mitigating the immunosuppressive tumor microenvironment effectively limits systemic disease progression.

Metastatic assessment in Lung and Liver tissue (Mean ± SD)

Groups	Average foci in Lung per slide	Size of foci in lung (µm)	No of foci in liver per field
Control	7.2 ± 3.1	696 ± 193	52.7 ± 8.5
Pirfenidone	4.5 ± 2.1	711 ± 247	48 ± 6.8
Anti-PD-1	6.2 ± 0.8	725 ± 293	30.8 ± 4
Combination	1.3 ± 1.0	273 ± 259	26.3 ± 6

Animal Survival and Ethical Endpoint Monitoring.

No statistically significant differences in survival were observed among the Pirfenidone-treated, anti-PD-1 antibody-treated, or combination-treated groups compared with the respective control groups in either the CT26 or 4T1 tumor-bearing mouse models throughout the 21-day treatment period. Furthermore, all animals remained within the predefined ethical and humane endpoint criteria during the study, with no mortality recorded. Therefore, survival analysis and Kaplan–Meier survival curves were not performed

Pirfenidone in combination with Anti-PD-1 Treatment improves tumor Immune Microenvironment in 4T1 Mice

Analysis of tumor cytokine levels in the 4T1 model revealed no statistically significant changes in TNF-α or IL-6 protein levels following treatment with Pirfenidone, anti-PD-1 antibody, or their combination compared with the vehicle control group. However, IFN-γ levels were significantly increased only in the Pirfenidone plus anti-PD-1 combination group, suggesting enhanced antitumor immune activation. In contrast, TGF-β levels were significantly reduced in both the Pirfenidone monotherapy and combination treatment groups, indicating a potential attenuation of the immunosuppressive tumor microenvironment.

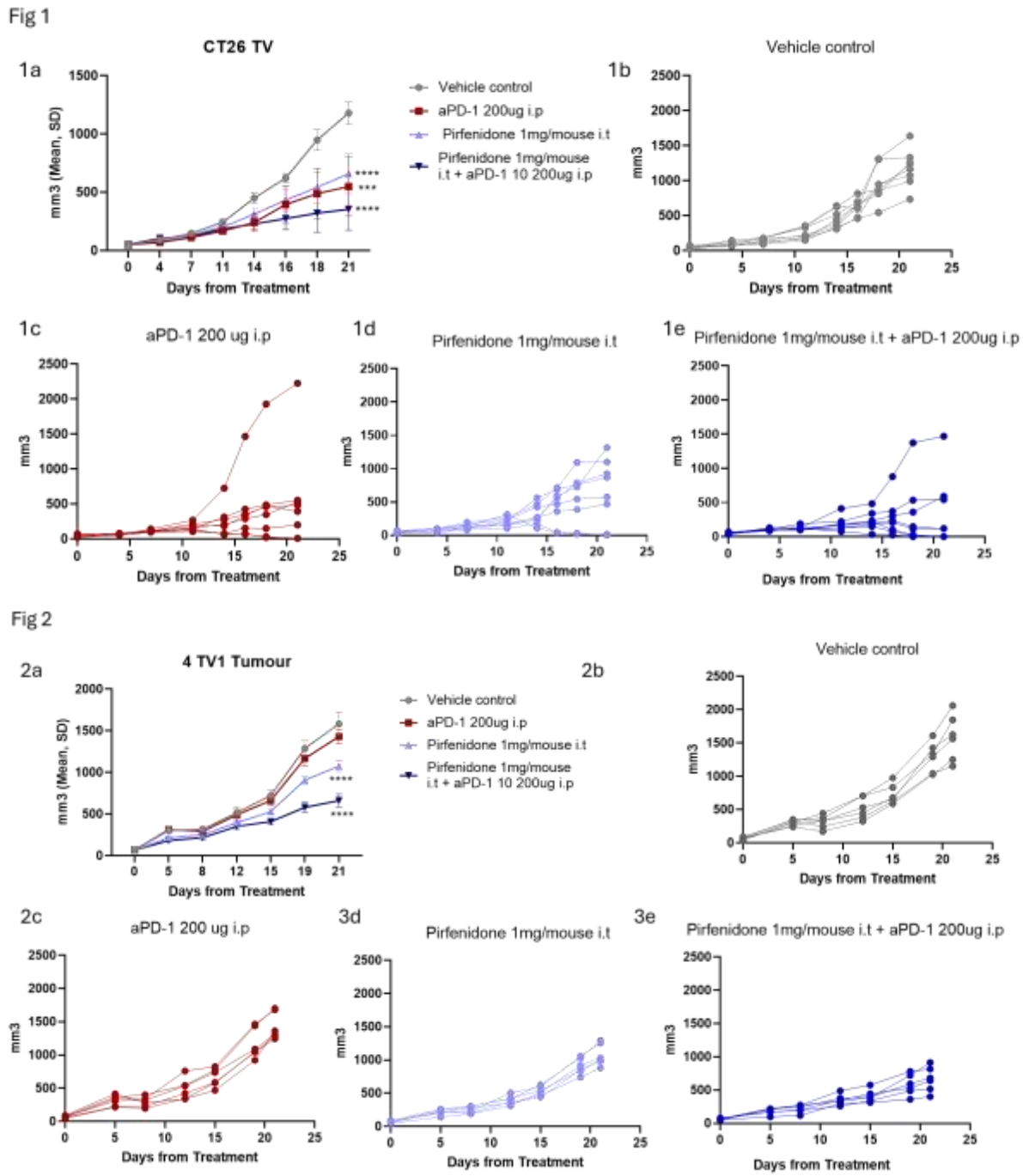

Figure 1&2. Combination therapy demonstrates additive antitumor effects and reduces tumor growth.

(1a-1e) Tumor growth curves of CT26 and individual group growth kinetics and (2a-2e) Tumor growth curves of 4T1 and individual group growth kinetics following treatment with vehicle control, anti–PD-1 antibody (200µg/mouse, intraperitoneal), pirfenidone (1 mg/mouse, intratumoral), or the combination. Tumor volumes are shown as mean ± SD. Statistical significance was assessed by using a two-way repeated measures analysis of variance (ANOVA) and Post-hoc comparisons were performed using Dunnett's multiple comparisons test. p values are indicated as follows: $p< 0.05$ (*), $p < 0.01$ (**), $p < 0.001$ (***), $p< 0.0001$ (****)

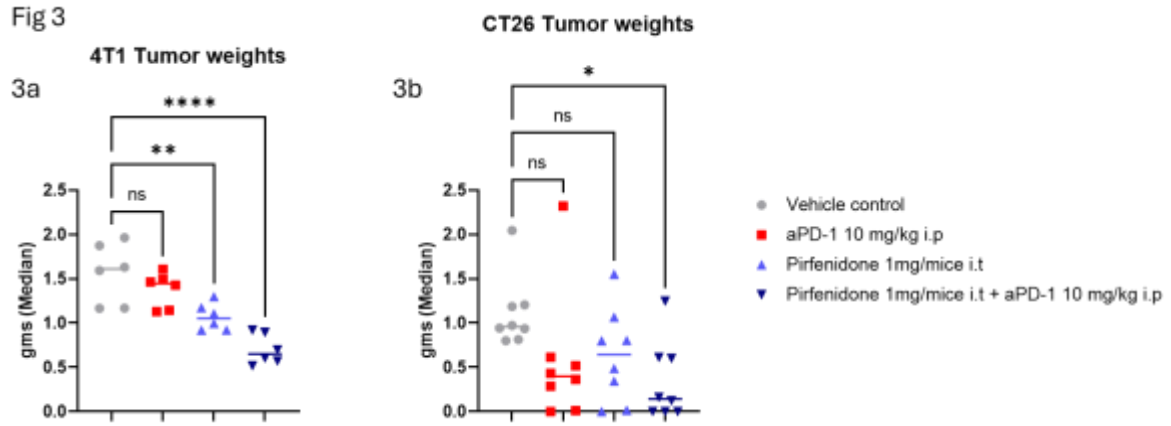

Figure 3. CT26 and 4T1 tumor weights on day 21 post treatment initiation.

3a and 3b represent 4T1 and CT26 tumor weights in gms on day 21 post treatment initiation, and data were presented as median values with individual points. Statistical comparisons were performed using ordinary one-way ANOVA followed by Dunnett's post-hoc multiple comparisons test. p values are indicated as follows: ns = not significant; p< 0.05 (*), p < 0.01 (**), p < 0.001 (***), p< 0.0001 (****)

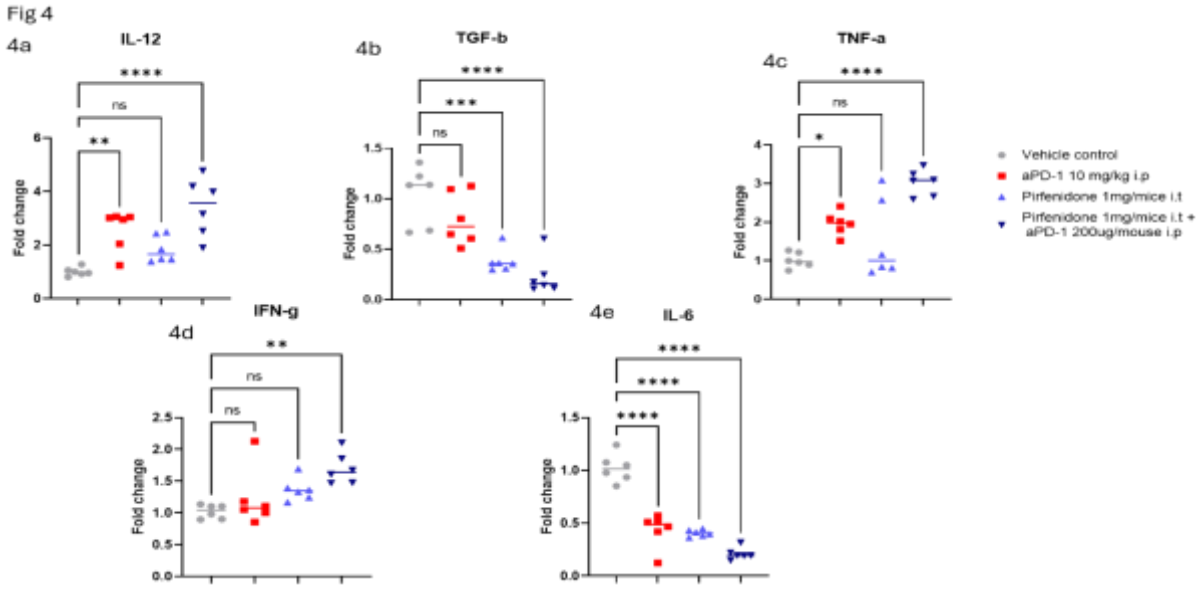

Figure 4. Effect of monotherapies and combination on tumor cytokine gene expression.

(a, e) Data was presented as fold change relative to the vehicle control of IL-12 (a), TGF-β (b) TNF-α (c), IFN-γ (d) and IL-6 (e) in tumor tissues, normalized to GAPDH. Statistical comparisons were performed using ordinary one-way ANOVA. p values are indicated as follows: ns = not significant; p< 0.05 (*), p < 0.01 (**), p < 0.001 (***), p< 0.0001 (****)

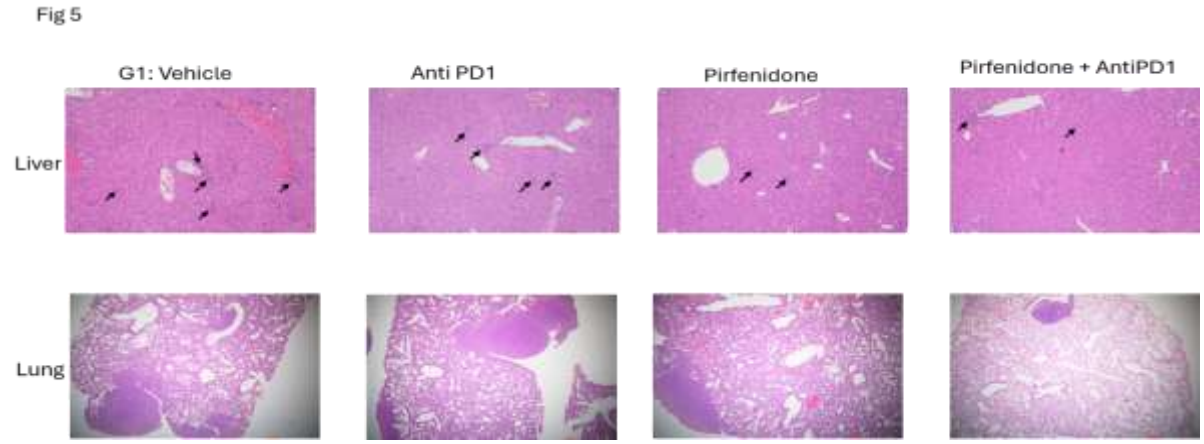

Figure 5. Effect of monotherapies and combination on tumor metastasis in Lung and Liver.

Photographs showing macroscopically visible metastatic nodules indicated by black arrows in Liver (100x magnification) and Lungs (40× magnification) of mice across treatment groups.

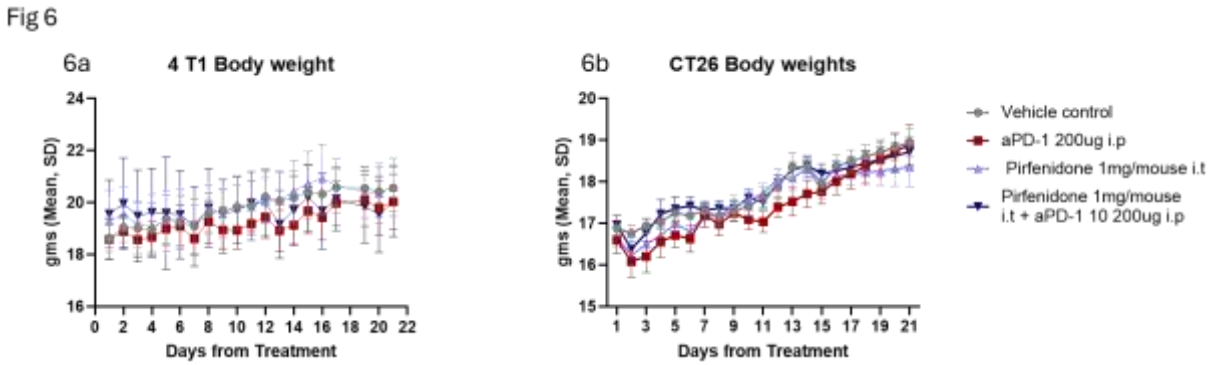

Figure 6. Effect of monotherapies and combination on body weights.

(a, b) Body weight curves of CT26 and 4T1 studies following treatment with vehicle control, anti–PD-1 antibody (200µg/mouse, intraperitoneal), pirfenidone (1 mg/mouse, intratumoral), or the combination. Tumor volumes are shown as mean ± SD. Statistical significance was assessed by two-way ANOVA with Dunnett post hoc analysis

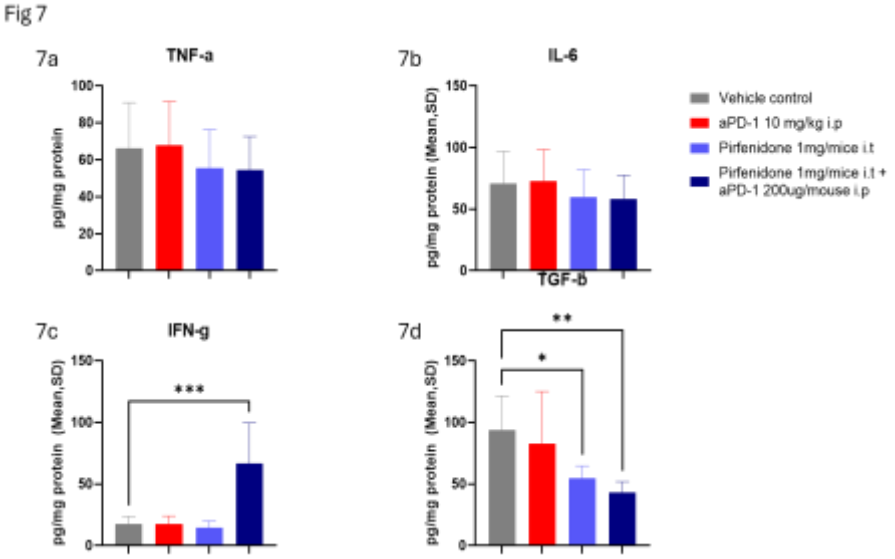

Figure 7. Intratumoral cytokine profiles across treatment groups.

(a, d) Data was presented as mean, SD of TNF-a (a), IL-6 (b), IFN γ (c) and TGF-β (d)in tumor tissues, normalized to total protein. Statistical comparisons were performed using ordinary one way ANOVA. p values are indicated as follows: ns = not significant; p< 0.05 (*), p < 0.01 (**), p < 0.001 (***), p< 0.0001 (****)

DISCUSSION

This study demonstrates that intratumoral pirfenidone administration, alone and particularly in combination with anti-PD-1 antibodies, produces significant antitumor effects in immunocompetent syngeneic CT26 and 4T1 mouse models. The synergistic benefits of combination therapy suggest complementary mechanisms of action involving both TME remodeling and enhanced immune checkpoint inhibition.

Pirfenidone-Mediated Tumor Microenvironment Remodeling

Pirfenidone's antitumor effects appear to be mediated through multiple mechanisms. First, the compound inhibits TGF-β signaling via suppression of p-Smad2/3 and reduction in TGF-β expression[22]. This finding aligns with recent reports demonstrating that TGF-β pathway inhibition diminishes CAF activation and reduces stromal fibrosis[23]. The observed reduction in α-SMA expression supports the hypothesis that pirfenidone promotes a shift from activated, immunosuppressive fibroblasts toward a less activated phenotype. Such structural modification of the stroma is critical, as CAFs are frequently more competent than lung-derived fibroblasts at fostering tumor progression through the release of growth factors and immune modulators [24].

Second, pirfenidone treatment significantly reduced IL-6 and TGF-β expression, both known MDSC-recruiting chemokines and cytokines[25]. This is particularly significant because MDSC-mediated immune suppression represents a major barrier to anti-PD-1 efficacy[26]. Consequently, the ability of pirfenidone to attenuate these stromal constraints facilitates deeper effector cell penetration into the tumor parenchyma [27,28]. This enhanced infiltration is associated with increased CD8+ T effector cell activity, which synergizes with anti-PD-1 therapy to overcome the immune exclusion

characteristic of highly fibrotic tumors [29]. These observations are consistent with studies indicating that targeted stromal modulation can enhance the efficacy of immune checkpoint blockade by mitigating the inhibitory signaling pathways maintained by cancer-associated fibroblasts [30,31].

Third, the enhancement of pro-inflammatory cytokine expression (TNF-α, IFN-γ, IL-12) and IFN-γ protein suggests that pirfenidone treatment creates a more permissive environment for CD8+ T cell activation and function. The significant increase in cytokine expression in combination-treated tumors demonstrates that TME remodeling promotes T cell recruitment, consistent with published findings[12].

The relationship between TGF-β-driven stromal remodeling and T cell exclusion has been elegantly demonstrated in landmark studies showing that TGF-β signaling within the CAF compartment physically prevents T cell penetration into tumor nests, even in the presence of an active peripheral immune response[28,32]. This TGF-β-mediated exclusion mechanism is distinct from PD-1-mediated T cell dysfunction and operates independently of checkpoint pathways, explaining why a substantial proportion of patients with TGF-β-high tumors fail to respond to PD-1/PD-L1 blockade as monotherapy[28]. By attenuating this exclusion mechanism, pirfenidone may convert tumors from an immune-excluded to an immune-inflamed phenotype that is more permissive to checkpoint inhibitor efficacy[33]. Furthermore, such a shift in the tumor microenvironment underscores the necessity of targeting the fibrotic stroma to overcome the limitations of current immunotherapies, as CAFs can actively neutralize the impact of immune checkpoint inhibitors through the secretion of diverse inhibitory molecules [34,35].

Synergistic Combination Effects

The superior efficacy of combination therapy compared to monotherapies suggests that pirfenidone-induced TME remodeling enhances checkpoint inhibitor responsiveness. This additive effect is mechanistically plausible: pirfenidone reduces the fibrotic barrier and immunosuppressive microenvironment, potentially increasing T cell accessibility to tumor-resident PD-1+ lymphocytes that are targets of anti-PD-1 blockade. Furthermore, the depletion of inhibitory factors like CXCL12 or prostaglandin E2 by modified stromal cells may further augment the cytotoxic potential of these recruited T cells, reinforcing the therapeutic efficacy of combination regimens [36,37]. Additionally, evidence suggests that mitigating the desmoplastic stroma can enhance the efficacy of chemotherapy and immunotherapy alike by improving the therapeutic index of infiltrating immune cells [38,39].

Notably, recent findings indicate that antagonizing TGF-β signaling not only facilitates T cell infiltration but also effectively reverses the resistance of immune-excluded tumors to anti-PD-1/PD-L1 therapy [32,40]. By neutralizing these barriers, simultaneous targeting of both TGF-β and PD-L1 can result in marked tumor regression, providing a robust rationale for combining anti-fibrotic agents with checkpoint blockade [41,42].

Future studies employing targeted MDSC depletion or adoptive transfer experiments would directly examine the mechanistic contribution of MDSC reduction to combination therapy efficacy and could identify predictive biomarkers for patient stratification. Moreover, ongoing investigations into the heterogeneity of cancer-associated fibroblasts may further elucidate whether specific subpopulations are more susceptible to pirfenidone-induced phenotypic modulation [43].

Clinical Implications and Translational Potential

These preclinical findings have important clinical implications. Specifically, pirfenidone—an FDA-approved antifibrotic for idiopathic pulmonary fibrosis with a well-characterized tolerability profile characterized by predominantly mild-to-moderate gastrointestinal and dermatological adverse events[44–46]—provides a clinically viable agent to integrate into oncology protocols, priming resistant desmoplastic tumors for enhanced immune checkpoint inhibitor responsiveness.

Recent clinical trials combining anti-fibrotic agents with checkpoint inhibitors in lung cancer patients show encouraging preliminary results, supporting the clinical relevance of our approach[47]. Furthermore, the potential for repurposing established anti-fibrotics, such as those targeting the TGF-β1/Smad/CTGF pathway, offers a pragmatic strategy to modulate the tumor microenvironment without the risks associated with novel experimental agents [48].

The intratumoral delivery strategy deserves additional consideration as an emerging paradigm in cancer immunotherapy. Moreover, intratumoral immunotherapy platforms have demonstrated that local intervention can elicit systemic anti-tumor responses through the priming of tumor-reactive T cells that circulate and exert anti-tumor effects at distant sites — the so-called abscopal effect[49]. Localized treatments such as intratumoral delivery improve overall efficacy by achieving supraphysiological drug concentrations directly within the tumor microenvironment, thereby enhancing stromal remodeling, T cell infiltration, and synergy with systemic anti-PD-1 while reducing systemic toxicity compared to oral or intravenous administration[49]. This approach minimizes off-target effects, such as the gastrointestinal and dermatological adverse events associated with systemic pirfenidone[44–46]Whether the combination of intratumoral pirfenidone and systemic anti-PD-1 therapy can elicit such systemic responses in our model warrants further investigation, but represents a compelling area for future study. From a translational standpoint, intratumoral administration is clinically feasible for accessible tumors and is already utilized in approved therapies such as talimogene laherparepvec for melanoma, providing a regulatory and logistical precedent for this approach[49].

However, important considerations for clinical translation include: (1) optimization of pirfenidone dosing and administration schedule; (2) patient stratification based on tumor fibrosis and immune infiltration; (3) comprehensive safety profiling in combination with PD-1 antibodies; and (4) evaluation in additional tumor histologies and models with variable immunogenicity.

Limitations

This study has several limitations. First, tumor growth was measured only by caliper, which may underestimate internal tumor heterogeneity. Future studies should incorporate magnetic resonance imaging or micro-computed tomography for more precise volumetric assessment. Second, this study evaluated only a single anti-PD-1 antibody clone; evaluation of other checkpoint modulators (anti-PD-L1, anti-CTLA-4) would strengthen conclusions regarding generalizability. Third, mechanistic studies were limited to day-21 endpoints; kinetic studies examining immune infiltration at multiple time points would provide mechanistic clarity. Fourth, this study did not evaluate long-term toxicity or autoimmune sequelae; extended monitoring of surviving animals would be important. Finally, this study did not perform a quantitative assessment of tumor fibrosis, such as histological analysis of collagen deposition, which would be necessary to directly correlate stromal remodeling with therapeutic outcomes

CONCLUSIONS

This preclinical study provides compelling evidence that intratumoral pirfenidone synergizes with anti-PD-1 antibodies to produce superior antitumor efficacy compared to monotherapy in CT26 and 4T1 syngeneic models. The combination approach appears to work through complementary mechanisms: pirfenidone-mediated TME remodeling and TGF-β pathway inhibition, combined with PD-1 checkpoint blockade-enhanced T cell function.

Future Directions

Future studies should investigate: (1) systemic pirfenidone dosing and administration routes; (2) combination with other immunotherapies including CAR-T cells or therapeutic cancer vaccines; (3) mechanistic studies employing single-cell RNA sequencing to characterize immune and stromal cell populations; (4) efficacy in additional immunologically "cold" tumor models; and (5) toxicity and immunogenicity studies in larger animal models prior to human clinical trials.

Author Contribution

CH Sandeep Reddy: Conceptualization, Methodology, Data Collection, Formal Analysis, Writing – Original Draft
Repudi Lalitha: Conceptualization, Writing – Review & Editing, Supervision

REFERENCES

1. Lind H, Gameiro SR, Jochéms C, Donahue RN, Strauss J, Gulley JL, Palena C, Schlom J. Dual targeting of TGF-β and PD-L1 via a bifunctional anti-PD-L1/TGF-βRII agent: status of preclinical and clinical advances. Journal for ImmunoTherapy of Cancer 2020;8. https://doi.org/10.1136/jitc-2019-000433 .
2. Nowicki TS, Hu-Lieskovan S, Ribas A. Mechanisms of Resistance to PD-1 and PD-L1 Blockade. The Cancer Journal 2018;24:47–53. https://doi.org/10.1097/ppo.0000000000000303 .
3. Liu Y, Sun Z. Turning cold tumors into hot tumors by improving T-cell infiltration. Theranostics 2021;11:5365–86. https://doi.org/10.7150/thno.58390 .
4. Wang M, Wang S, Desai J, Trapani JA, Neeson PJ. Therapeutic strategies to remodel immunologically cold tumors. Clinical & Translational Immunology 2020;9. https://doi.org/10.1002/cti2.1226 .
5. Khosravi G, Mostafavi S, Bastan S, Ebrahimi N, Gharibvand RS, Eskandari N. Immunologic tumor microenvironment modulators for turning cold tumors hot. Cancer Communications 2024;44:521–53. https://doi.org/10.1002/cac2.12539 .
6. Yi M, Li T, Niu M, Zhang H, Wu Y, Wu K, Dai Z. Targeting cytokine and chemokine signaling pathways for cancer therapy. Signal Transduction and Targeted Therapy 2024;9:176–176. https://doi.org/10.1038/s41392-024-01868-3 .
7. Hou A, Hou K, Huang Q, Lei Y, Chen W-L. Targeting Myeloid-Derived Suppressor Cell, a Promising Strategy to Overcome Resistance to Immune Checkpoint Inhibitors. Frontiers in Immunology 2020;11:783–783. https://doi.org/10.3389/fimmu.2020.00783 .
8. Monteran L, Erez N. The Dark Side of Fibroblasts: Cancer-Associated Fibroblasts as Mediators of Immunosuppression in the Tumor Microenvironment. Frontiers in Immunology 2019;10:1835–1835. https://doi.org/10.3389/fimmu.2019.01835 .
9. Liu T, Han C, Wang S, Fang P, Ma Z, Xu L, Yin R. Cancer-associated fibroblasts: an emerging target of anti-cancer immunotherapy. Journal of Hematology & Oncology 2019;12:86–86. https://doi.org/10.1186/s13045-019-0770-1 .
10. Schaefer C, Ruhrmund D, Pan L, Seiwert SD, Kossen K. Antifibrotic activities of pirfenidone in animal models. European Respiratory Review 2011;20:85–97. https://doi.org/10.1183/09059180.00001111 .
11. Cannito S, Novo E, Parola M. Therapeutic pro-fibrogenic signaling pathways in fibroblasts. Advanced Drug Delivery Reviews 2017;121:57–84. https://doi.org/10.1016/j.addr.2017.05.017 .
12. Wan Q, Zou J, Huang Y, Liu C, Kang Y, Han H, Tang Y, Li L, Liu B, Zhao W, Yuan X. Pirfenidone facilitates immune infiltration and enhances the antitumor efficacy of PD-L1 blockade in mice. OncoImmunology 2020;9:1824631–1824631. https://doi.org/10.1080/2162402x.2020.1824631 .
13. Es HA, Zhand S, Thiery JP, Warkiani ME. Pirfenidone reduces immune-suppressive capacity of cancer-associated fibroblasts through targeting CCL17 and TNF-beta. Integrative Biology 2020;12:188–97. https://doi.org/10.1093/intbio/zyaa014 .
14. Zhu S, Zhang T, Zheng L, Liu H, Song W, Liu D, Li Z, Pan C. Combination strategies to maximize the benefits of cancer immunotherapy. Journal of Hematology & Oncology 2021;14:156–156. https://doi.org/10.1186/s13045-021-01164-5 .

15. Kim B, Malek E, Choi SH, Ignatz-Hoover JJ, Driscoll JJ. Novel therapies emerging in oncology to target the TGF-β pathway. Journal of Hematology & Oncology 2021;14:55–55. https://doi.org/10.1186/s13045-021-01053-x .
16. Zamarin D, Ricca J, Sadekova S, Oseledchyk A, Yu Y, Blumenschein WM, Wong J, Gigoux M, Merghoub T, Wolchok JD. PD-L1 in tumor microenvironment mediates resistance to oncolytic immunotherapy. Journal of Clinical Investigation 2018;128:1413–28. https://doi.org/10.1172/jci98047 .
17. Mediavilla-Varela M, Boateng KA, Noyes D, Antonia S. The anti-fibrotic agent pirfenidone synergizes with cisplatin in killing tumor cells and cancer-associated fibroblasts. BMC Cancer 2016;16. https://doi.org/10.1186/s12885-016-2162-z .
18. Pénzváltó Z, Chen JQ, Tepper CG, Davis RR, Silvestrini MT, Umeh-Garcia M, Sweeney C, Borowsky AD. A Syngeneic ErbB2 Mammary Cancer Model for Preclinical Immunotherapy Trials. Journal of Mammary Gland Biology and Neoplasia 2019;24:149–62. https://doi.org/10.1007/s10911-019-09425-3 .
19. Hong X, Ma M, Cui H, Yang X, Li F, Chu M, Ye Y, Jiang Z, Pei L, Liu S, Xie Y. PD-1 blockade elicits a systemic immune response but not in the tumor of TNBC mice. Acta Biochimica et Biophysica Sinica 2025. https://doi.org/10.3724/abbs.2025240 .
20. Pedersen IS, Orfin K, Nielsen K, Holst P. P02.05 Investigation of a syngeneic a-PD-1 antibody to treat murine 4T1 mammary carcinoma 2020. https://doi.org/10.1136/jitc-2020-itoc7.40 .
21. Snipstad S, Bremnes F, Haugum MD, Sulheim E. Characterization of immune cell populations in syngeneic murine tumor models. Cancer Medicine 2023;12:11589–601. https://doi.org/10.1002/cam4.5784 .
22. Wang G, Zhou X, Guo Z, Huang N, Li J, Lv Y-F, Han L, Zheng W, Xu D, Chai D, Li H, Li L, Zheng J. The Anti-fibrosis drug Pirfenidone modifies the immunosuppressive tumor microenvironment and prevents the progression of renal cell carcinoma by inhibiting tumor autocrine TGF-β. Cancer Biology & Therapy 2022;23:150–62. https://doi.org/10.1080/15384047.2022.2035629 .
23. Grauel AL, Nguyen B, Ruddy DA, Laszewski T, Schwartz S, Chang J, Chen J, Piquet M, Pelletier MR, Zheng Y, Kirkpatrick ND, Wu J, Weck A de, Riester M, Hims M, Geyer FC, Wagner JP, MacIsaac KD, Deeds J, Diwanji R, Jayaraman P, Yu Y, Simmons Q, Weng S, Raza A, Minie B, Dostalek M, Chikkegowda P, Ruda VM, Iartchouk O, Chen N, Thierry R, Zhou J, Pruteanu-Malinici I, Fabre C, Engelman JA, Dranoff G, Cremasco V. TGFβ-blockade uncovers stromal plasticity in tumors by revealing the existence of a subset of interferon-licensed fibroblasts. Nature Communications 2020;11. https://doi.org/10.1038/s41467-020-19920-5 .
24. Fujiwara A, Funaki S, Fukui E, Kimura K, Kanou T, Ose N, Minami M, Shintani Y. Effects of pirfenidone targeting the tumor microenvironment and tumor-stroma interaction as a novel treatment for non-small cell lung cancer. Scientific Reports 2020;10. https://doi.org/10.1038/s41598-020-67904-8 .
25. Lv Q, Wang J, Xu C, Huang X, Ruan Z, Dai Y. Pirfenidone alleviates pulmonary fibrosis in vitro and in vivo through regulating Wnt/GSK-3β/β-catenin and TGF-β1/Smad2/3 signaling pathways. Molecular Medicine 2020;26. https://doi.org/10.1186/s10020-020-00173-3 .
26. Li Y, Ru Y, Huang X, Chen C, Dou D, Wang Q, Wu X, Liu H, Sun T. Chrysin targets myeloid-derived suppressor cells and enhances tumour response to anti-PD-1 immunotherapy. Clinical and Translational Medicine 2022;12. https://doi.org/10.1002/ctm2.1019 .
27. Zhou M, Wang J, Pan J, Wang H, Huang L, Hou B, Lai Y, Wang F, Guan Q, Wang F, Xu Z, Yu H. Nanovesicles loaded with a TGF-β receptor 1 inhibitor overcome immune resistance to potentiate cancer immunotherapy. Nature Communications 2023;14. https://doi.org/10.1038/s41467-023-39035-x .
28. Mariathasan S, Turley SJ, Nickles D, Castiglioni A, Yuen K, Wang Y, Kadel EE, Koeppen H, Astarita JL, Cubas R, Jhunjhunwala S, Banchereau R, Yang Y, Guan Y, Chalouni C, Ziai J, Şenbabaoğlu Y, Santoro SP, Sheinson D, Hung J, Giltnane JM, Pierce AA, Mesh K, Lianoglou S, Riegler J, Carano RAD, Eriksson P, Höglund M, Somarriba L, Halligan DL, Heijden MS van der, Loriot Y, Rosenberg JE, Fong L, Mellman I, Chen DS, Green M, Derleth CL, Fine G, Hegde PS, Bourgon R, Powles T. TGFβ attenuates tumour response to PD-L1 blockade by contributing to exclusion of T cells. Nature 2018;554:544–8. https://doi.org/10.1038/nature25501 .
29. Pei L, Liu Y, Liu L, Gao S, Gao X, Feng Y, Sun Z, Zhang Y, Wang C. Roles of cancer-associated fibroblasts (CAFs) in anti- PD-1/PD-L1 immunotherapy for solid cancers. Molecular Cancer 2023;22. https://doi.org/10.1186/s12943-023-01731-z .
30. Takai K, Le A, Weaver VM, Werb Z. Targeting the cancer-associated fibroblasts as a treatment in triple-negative breast cancer. Oncotarget 2016;7:82889–901. https://doi.org/10.18632/oncotarget.12658 .
31. Kato R, Haratani K, Hayashi H, Sakai K, Sakai H, Kawakami H, Tanaka K, Takeda M, Yonesaka K, Nishio K, Nakagawa K. Nintedanib promotes antitumour immunity and shows antitumour activity in combination with PD-1 blockade in mice: potential role of cancer-associated fibroblasts. British Journal of Cancer 2020;124:914–24. https://doi.org/10.1038/s41416-020-01201-z .
32. Tauriello DVF, Palomo-Ponce S, Stork D, Berenguer A, Badia-Ramentol J, Iglesias M, Sevillano M, Ibiza S, Cañellas-Socias A, Hernando-Momblona X, Byrom D, Matarin JA, Calon A, Rivas E, Nebreda ÁR, Riéra A, Attolini CS, Batlle E. TGFβ drives immune evasion in genetically reconstituted colon cancer metastasis. Nature 2018;554:538–43. https://doi.org/10.1038/nature25492 .
33. Chen DS, Mellman I. Elements of cancer immunity and the cancer–immune set point. Nature 2017;541:321–30. https://doi.org/10.1038/nature21349 .
34. Gieniec KA, Butler LM, Worthley DL, Woods SL. Cancer-associated fibroblasts—heroes or villains? British Journal of Cancer 2019;121:293–302. https://doi.org/10.1038/s41416-019-0509-3 .

35. Linares J, Marín-Jiménez JA, Badia-Ramentol J, Calon A. Determinants and Functions of CAFs Secretome During Cancer Progression and Therapy. Frontiers in Cell and Developmental Biology 2021;8. https://doi.org/10.3389/fcell.2020.621070 .
36. Piersma B, Hayward M-K, Weaver VM. Fibrosis and cancer: A strained relationship. Biochimica et Biophysica Acta (BBA) - Reviews on Cancer 2020;1873:188356–188356. https://doi.org/10.1016/j.bbcan.2020.188356 .
37. Tang T, Huang X, Zhang G, Hong Z, Bai X, Liang T. Advantages of targeting the tumor immune microenvironment over blocking immune checkpoint in cancer immunotherapy. Signal Transduction and Targeted Therapy 2021;6. https://doi.org/10.1038/s41392-020-00449-4 .
38. Prakash J, Shaked Y. The Interplay between Extracellular Matrix Remodeling and Cancer Therapeutics. Cancer Discovery 2024;14:1375–88. https://doi.org/10.1158/2159-8290.cd-24-0002 .
39. Kim DK, Jeong J, Lee DS, Hyeon DY, Park GW, Jeon S, Lee KB, Jang J, Hwang D, Kim HM, Jung K. PD-L1-directed PlGF/VEGF blockade synergizes with chemotherapy by targeting CD141+ cancer-associated fibroblasts in pancreatic cancer. Nature Communications 2022;13. https://doi.org/10.1038/s41467-022-33991-6 .
40. Yi M, Li T, Niu M, Wu Y, Zhao Z, Wu K. TGF-β: A novel predictor and target for anti-PD-1/PD-L1 therapy. Frontiers in Immunology 2022;13. https://doi.org/10.3389/fimmu.2022.1061394 .
41. Yang W, Liu S, Mao M, Gong Y, Li X, Lei T, Liu C, Wu S, Hu Q. T-cell infiltration and its regulatory mechanisms in cancers: insights at single-cell resolution. Journal of Experimental & Clinical Cancer Research 2024;43. https://doi.org/10.1186/s13046-024-02960-w .
42. Chakravarthy A, Khan L, Bensler NP, Bose P, Carvalho DDD. TGF-β-associated extracellular matrix genes link cancer-associated fibroblasts to immune evasion and immunotherapy failure. Nature Communications 2018;9. https://doi.org/10.1038/s41467-018-06654-8 .
43. Hauge A, Rofstad EK. Antifibrotic therapy to normalize the tumor microenvironment. Journal of Translational Medicine 2020;18. https://doi.org/10.1186/s12967-020-02376-y .
44. Valeyre D, Albera C, Bradford WZ, Costabel U, King TE, Leff JA, Noble PW, Sahn SA, Bois RM du. Comprehensive assessment of the long-term safety of pirfenidone in patients with idiopathic pulmonary fibrosis. Respirology 2014;19:740–7. https://doi.org/10.1111/resp.12297 .
45. Lancaster L, Andrade JA de, Zibrak JD, Padilla ML, Albera C, Nathan SD, Wijsenbeek M, Stauffer JL, Kirchgaessler K-U, Costabel U. Pirfenidone safety and adverse event management in idiopathic pulmonary fibrosis. European Respiratory Review 2017;26:170057–170057. https://doi.org/10.1183/16000617.0057-2017 .
46. Bonella F, Spagnolo P, Ryerson CJ. Current and Future Treatment Landscape for Idiopathic Pulmonary Fibrosis. Drugs 2023;83:1581–93. https://doi.org/10.1007/s40265-023-01950-0 .
47. Huang C, Wick J, Komiya T. Preliminary results of atezolizumab and pirfenidone in non-small cell lung cancer. Journal of Clinical Oncology 2024;42. https://doi.org/10.1200/jco.2024.42.16_suppl.e15197 .
48. Darragh LB, Oweida A, Karam SD. Overcoming Resistance to Combination Radiation-Immunotherapy: A Focus on Contributing Pathways Within the Tumor Microenvironment. Frontiers in Immunology 2019;9. https://doi.org/10.3389/fimmu.2018.03154 .
49. Marabelle A, Tselikas L, Baère T de, Houot R. Intratumoral immunotherapy: using the tumor as the remedy. Annals of Oncology 2017;28. https://doi.org/10.1093/annonc/mdx683 .